IOPscience iopscience.iop.org

Home Search Collections Journals About Contact us My IOPscience

The use of gold nanoparticles to enhance radiotherapy in mice

This article has been downloaded from IOPscience. Please scroll down to see the full text article.

2004 Phys. Med. Biol. 49 N309

(http://iopscience.iop.org/0031-9155/49/18/N03)

View the table of contents for this issue, or go to the journal homepage for more

Download details:
IP Address: 155.37.245.170
The article was downloaded on 19/08/2013 at 15:47

Please note that terms and conditions apply.

INSTITUTE OF PHYSICS PUBLISHING PHYSICS IN MEDICINE AND BIOLOGY

Phys. Med. Biol. **49** (2004) N309–N315 PII: S0031-9155(04)81626-9

NOTE

The use of gold nanoparticles to enhance radiotherapy in mice

James F Hainfeld[1], Daniel N Slatkin[1] and Henry M Smilowitz[2]

[1] Nanoprobes, Inc., 95 Horse Block Rd., Yaphank, NY 11980, USA
[2] Department of Pharmacology, University of Connecticut Health Center, 263 Farmington Ave., Farmington, CT 06030, USA

E-mail: hainfeld@nanoprobes.com and smilowitz@nso1.uchc.edu

Received 1 June 2004
Published 3 September 2004
Online at stacks.iop.org/PMB/49/N309
doi:10.1088/0031-9155/49/18/N03

Abstract

Mice bearing subcutaneous EMT-6 mammary carcinomas received a single intravenous injection of 1.9 nm diameter gold particles (up to 2.7 g Au/kg body weight), which elevated concentrations of gold to 7 mg Au/g in tumours. Tumour-to-normal-tissue gold concentration ratios remained ∼8:1 during several minutes of 250 kVp x-ray therapy. One-year survival was 86% versus 20% with x-rays alone and 0% with gold alone. The increase in tumours safely ablated was dependent on the amount of gold injected. The gold nanoparticles were apparently non-toxic to mice and were largely cleared from the body through the kidneys. This novel use of small gold nanoparticles permitted achievement of the high metal content in tumours necessary for significant high-Z radioenhancement.

1. Introduction

Dose enhancement at interfaces between high and low atomic number (Z) materials has been studied for over 50 years (Spiers 1949). This effect caused burns and necrosis in tissue around reconstructive wires in mandibular cancer patients after radiation treatments (Castillo *et al* 1988). The concept of using high-Z materials for dose enhancement in cancer radiotherapy was advanced over 20 years ago by Matsudaira *et al* (1980), who measured a radioenhancing effect of iodine on cultured cells. Nath *et al* (1990) incorporated iodine into cellular DNA with iododeoxyuridine *in vitro*, and found a radiation enhancement of ∼3. Regulla *et al* (1998) showed a physical dose enhancement factor of ∼100 within a range of 10 μm and a biological enhancement factor of up to 50 for fibroblast monolayers irradiated on a gold foil. Herold *et al* (2000) injected 1.5–3.0 μm gold particles directly into a tumour followed by irradiation and found that excised cells had reduced plating efficiency. Santos Mello *et al* (1983) found that direct tumour injection of iodine contrast medium followed

 © 2004 IOP Publishing Ltd Printed in the UK

by 100 kVp x-rays completely suppressed the growth of 80% of tumours in mice. Norman *et al* (1997) modified a CT scanner to deliver tomographic orthovoltage (140 kVp) x-rays to spontaneous canine brain tumours after intravenous injection with iodine contrast medium, which resulted in 53% longer survival. This apparatus was then used in a phase I human trial of brain tumours using intravenous injection of iodine contrast medium, which demonstrated the method to be safe and potentially beneficial (Rose *et al* 1999). Synchrotron radiation has also been tested in combination with intratumourally injected cisplatin drug therapy for treating brain tumours in rats (Biston *et al* 2004). We have extended these concepts by using novel gold nanoparticles to deliver a very large quantity of gold to tumours via intravenous injection without apparent toxicity. Combination with x-rays resulted in eradication of most tumours.

2. Materials and methods

Animals and tumours. Balb/C mice were injected subcutaneously in the thigh with 10^6 EMT-6 syngeneic mammary carcinoma cells (Rockwell *et al* 1972) suspended in 0.05 ml of equal volumes of medium and Matrigel. Tumours grew to 50–90 mm^3 in about 1 week. Tumour volume was estimated as half of the small diameter squared times the large diameter (Rofstad and Brustad 1985). Gold nanoparticles were injected via a tail vein. Experimental protocols using animals were approved by the University of Connecticut Health Center animal care committee.

Gold nanoparticles. 1.9 ± 0.1 nm gold nanoparticles, preparation no 1101, were obtained from Nanoprobes, Inc. (Yaphank, New York). The size of the nanoparticles was determined by electron microscopy. The concentration of injected gold was 270 mg Au/cc for the 2.7 g Au/kg case and 135 mg Au/cc for the 1.35 g Au/kg case, and the volume injected was 0.01 ml per g mouse weight. Nanoparticles were suspended in phosphate-buffered saline at pH 7.4.

Irradiation. Approximately 2 min post injection, a 1 inch diameter region of the leg containing the tumour was irradiated with 250 kVp x-rays through a Thoreaus-1 filter at 5 Gy min^{-1} using a Siemens Stabilipan x-ray generator.

Statistics. Wilcoxon non-parametric two-sample rank-sum analysis was used.

Gold analysis of tissues. Tissues were excised, placed in tared vials and analysed for gold by graphite furnace atomic absorption spectrometry.

Radiographs. A Lorad Medical Systems, Inc. mammography unit, model XDA101827 was used with 6 s exposures taken at 22 kVp and 40 mA s.

Blood tests. Mice were killed two weeks after i.v. gold injection and 0.4 ml blood removed from the right ventricle. Analytes assayed were: haemoglobin, haematocrit, creatine, blood urea nitrogen, total protein, albumin, phosphorus, total bilirubin, direct bilirubin, gamma glutamyltransferase, aspartate aminotransferase, alanine aminotransferase, alkaline phosphatase.

3. Results

Syngeneic mouse mammary EMT-6 tumours were grown subcutaneously in the legs of mice. After intravenous injection of gold nanoparticles, the tumour region was irradiated with 250 kVp x-rays. The rate of tumour growth was dramatically different in mice receiving

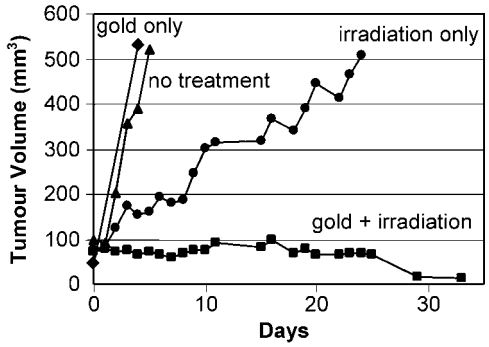

Figure 1. Average tumour volume after: (a) no treatment (triangles, $n = 12$); (b) gold only (diamonds, $n = 4$); (c) irradiation only (30 Gy, 250 kVp, circles, $n = 11$); (d) intravenous gold injection (1.35 g Au/kg) followed by irradiation (squares, $n = 10$).

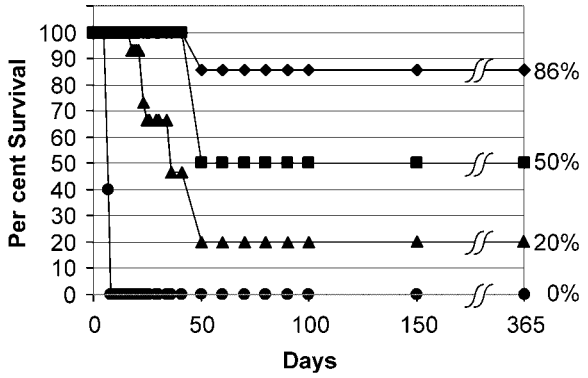

Figure 2. Graph of mice survival after various treatments of subcutaneous EMT-6 tumours. A gold dose response was evident. Circles: no treatment ($n = 17$), and gold only (1.35 g Au/kg, no irradiation), indistinguishable from no treatment ($n = 4$); triangles: irradiation only (26 Gy, 250 kVp), producing 20% long-term (>1 year) survival ($n = 15$); squares: irradiation after i.v. injection of 1.35 g Au/kg gold nanoparticles, 50% long-term survival ($n = 4$); diamonds: irradiation after 2.7 g Au/kg injection, producing 86% long-term survival ($n = 7$).

only radiation and those receiving gold followed by radiation. One month after mice received only x-ray therapy, all tumours grew to an average of more than five times their initial sizes. Concurrently, nine of ten similar mice that received 1.35 mg Au/g body weight shortly before the same x-ray therapy had no visible tumour; the tenth mouse had a tumour that was shrinking (figure 1). Administration of 1.35 g Au/kg without radiation did not retard tumour growth and had no therapeutic effect. The delivered dose was 30 Gy.

Because tumours that regress in the short term might regrow, an additional series of trials was done at a lower radiation dose (26 Gy) and responses followed for more than one year. Two levels of gold were administered, 1.35 and 2.70 g Au/kg body weight. Results are shown in a Kaplan–Meier survival graph (figure 2). All animals receiving either no radiation or gold without radiation died within two weeks. Irradiation alone slowed tumour growth and resulted in 20% long-term remissions. Those receiving injections of 1.35 or 2.7 g Au/kg before radiation showed 50% and 86% long-term (>1 year) survival, respectively. Combining the two groups given gold, the 'gold + radiation' group statistically differed from the 'radiation only' group with a certainty of >99% ($p < 0.01$).

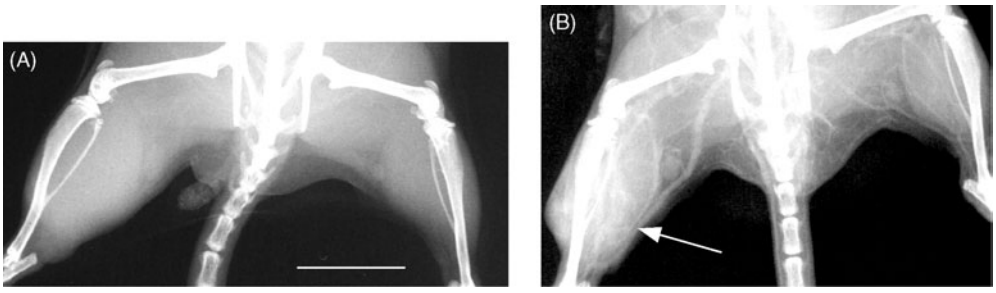

Figure 3. Radiographs of mouse hind legs before and after gold nanoparticle injection. (A) Before injection. (B) 2 min after i.v. gold injection (2.7 g Au/kg). Significant contrast (white) from the gold is seen in the leg with the tumour (arrow) compared with the normal contralateral leg. 6 s exposures at 22 kVp and 40 mA s. Bar = 1 cm.

When irradiation was started 2 min after injection of 2.7 g Au/kg, the blood content was 1.8 ± 0.1% gold by weight. Monte Carlo simulations using the EGS4 code (Nelson *et al* 1985) were used to estimate the dose to cells lining the vasculature carrying the gold. The simulations used the code's recent upgrades that include the LSCAT subroutine for low energy scattering (Namito *et al* 1995). A simple geometry was modelled with monochromatic x-rays incident on gold-water solutions of varying gold concentrations 0.85 cm thick followed by a pure water layer 1 cm thick. At the boundary between the gold and water solutions, 81 keV incident photons produced a dose increase for the 1.8% gold achieved *in vivo* of 550%, enough to cause catastrophic endothelial damage. Tumours in fact became haemorrhagic before shrinking.

A mammography x-ray unit was used to image the gold distribution in the tumour (figure 3). The radiograph taken before gold injection (figure 3(A)) shows bones and little soft tissue with no vascular detail. The tumour can only be vaguely recognized by the larger leg mass. However, after gold nanoparticle injection (figure 3(B)), many blood vessels become visible due to the gold absorption. Since the tumour has increased vascularity which is leaky, more gold nanoparticles and contrast appeared in the tumour (in leg with arrow in figure 3(B)) compared to the normal contralateral leg in figure 3(B).

Blood and tissue samples were analysed for gold. Pharmacokinetics showed an early rapid rise followed by a slower clearance rate. Gold in tumour peaked at 7.0 ± 1.6 min and fell to one-half of its peak value at 41.2 ± 19.5 min; gold in muscle peaked at 5.3 ± 0.6 min and fell to one-half at 24.2 ± 2.6 min. Thus, these gold nanoparticles cleared nearly twice as fast from normal muscle as from tumour. At 5 min following injection (the approximate midpoint of irradiation), the tumour-to-normal muscle Au ratio was 3.5:1.0 (table 1). The injected gold solution was dark black/brown, and at necropsy the periphery of some tumours was similarly dark. Upon analysis, these regions ('tumour periphery') showed almost twice the gold concentration of the main tumour mass ('tumour'). The periphery of one tumour contained 6.5 mg Au/g (12.0% i.d. Au/g), with a tumour-to-normal tissue ratio of 8.6.

With respect to preliminary toxicity testing, mice receiving 2.7 g Au/kg lived for more than one year without overt clinical signs. Analysis of blood from mice given 0.8 g Au/kg two weeks after injection showed haematocrits and enzymes within normal ranges.

4. Discussion

The size of gold particles (1.9 nm) was chosen to avoid high liver uptake (known for larger particles) and to take advantage of the 'leaky' vasculature of tumours (Dvorak *et al* 1988). In

Table 1. Biodistribution of gold 5 min post i.v. injection of 1.35 g Au/kg.

	% injected dose/g	Tumour-to-tissue ratio	Tumour periphery-to-tissue ratio
Tumour	4.9 ± 0.6	1.0	1.8
Tumour periphery	8.9 ± 3.2	0.6	1.0
Muscle	1.4 ± 0.1	3.5	6.4
Liver	2.8 ± 0.1	1.8	3.2
Kidney	132.0 ± 2.7	0.4	0.1
Blood	18.6 ± 3.7	0.3	0.5

fact, tumour uptake was 1.8 times that of liver per g tissue. Tumour specific extravasation is likely, since whole blood space in skeletal muscle is ∼2.3% (Cieslar *et al* 1998), and here muscle had 7.5% of the blood gold concentration (table 1), but the tumour periphery had 47.8% of the blood gold concentration. However, further studies are needed to distinguish extravasation from increased vascularization.

The method presented here appears to overcome many of the difficulties of previous attempts to use high-*Z* radioenhancement. Iododeoxyuridine treatment required approximately 22–45% of the thymine in cellular DNA to be substituted with iodouracil for a radiation enhancement of about 3 (Nath *et al* 1990). This would be difficult to achieve clinically and it is difficult to limit the replacement to only tumour cells. Gold foil enhancement (Regulla *et al* 1998) would not be easily adaptable to uniform tumour treatment. Direct intratumoural injection of 1.5–3.0 μm gold particles upon histological examination showed no gold particles in zones of tightly packed tumour cells, suggesting that it would be difficult to achieve uniform delivery with particles of this size (Herold *et al* 2000). Iodine contrast media (Santos Mello *et al* 1983, Norman *et al* 1997, Rose *et al* 1999) have the disadvantage of low molecular weights and diffuse out of the normal vascular system rapidly, hindering tumour delivery. Gold nanoparticles have a longer blood half-life. The element gold also has a significant advantage over iodine in x-ray absorption with a higher K-edge farther from bone and soft tissue absorptions. A synchrotron was used by Biston *et al* (2004), where a striking synergy with the drug cisplatin was found. In that study direct intratumoural injection was used which always has the potential disadvantages of non-uniform delivery and lack of tumour specificity. By comparison, we achieved local concentrations in the tumour of 0.17 M gold after i.v. injection, whereas they achieved approximately 30 micromolar platinum, giving about a 5000 factor difference. The extremely low platinum concentration combined with their observation of no improvement in effect above versus below the K-edge of Pt would argue against a significant high-*Z* radioenhancement effect. The observed therapeutic results might be explained by the radiation improving penetration of the drug and the resulting improved pharmacological effect. Higher platinum concentrations are limited by the systemic toxicity of cisplatin.

Enhancement is optimal in the photoelectric-dominated x-ray spectrum (the gold K-edge is at 80.7 keV). 120 keV photons have a half-value layer of 4 cm, so application to deeper tumours (e.g., pancreatic and brain) needs to address potentially excessive entrance skin doses, perhaps by intraoperative radiation therapy or conformal (multidirectional) irradiation. Radioisotope brachytherapy (e.g., high-dose rate Ir-192) can be enhanced, and recent calculations indicate usefulness with megavoltage sources (Robar *et al* 2002). Direct intratumoural injection of diffusible gold may also be explored. A second-generation gold agent will have a targeting molecule (e.g., antibody) attached to further improve tumour

specificity. Although high-dose single-fraction irradiation is not generally optimal for clinical use, it was used here only to demonstrate the 'proof-of-principle' that systemically administered gold nanoparticles can significantly improve the *in vivo* efficacy of radiation therapy. The benefit from dose fractionation using this approach remains to be tested.

The high extinction coefficient of the gold particle, $\sim 3 \times 10^5$ M^{-1} at 420 nm, and its black colour at these high concentrations may make other modalities feasible, such as microwave, ultrasonic, infrared or laser heating (Pitsillides *et al* 2003, Hirsch *et al* 2003). This approach may also be useful in ablation of unwanted non-neoplastic tissues or cells.

5. Conclusion

This note demonstrates that intravenously administered small gold nanoparticles can deliver high levels of gold to tumours (up to 0.7% weight%) with specificity and thereby improve x-ray therapy. To our knowledge, this is the first demonstration of control of a malignant tumour *in vivo* through the preferential absorption of x-rays by high-Z nanoparticles.

Acknowledgments

We thank the following persons for their help: Michael Blewitt, Theresa Focella, Duane Hoch, Tigran Bacharian, J Robin Rice, PhD, Kashmiri L Chopra, Terry M Button, PhD, Lawrence E Reinstein, PhD, Bipin Jagjivan, MD, Robert J Dowsett, MD, Lahmer Lynds, PhD, Peter J Tutschka, MD, Richard C Shumway, MD. The research was supported in part by National Cancer Institute Small Business Innovative Research Phase 1 Grant 1R43CA83576-01.

References

Biston M-C, Joubert A, Adam J-F, Elleaume H, Bohic S, Charvet A M, Esteve F, Foray N and Balosso J 2004 Cure of Fisher rats bearing radioresistant F98 glioma treated with cis-platinum and irradiated with monochromatic synchrotron X-rays *Cancer Res.* **64** 2317–23

Castillo M H, Button T M, Doerr R, Homs M I, Pruett C W and Pearce J I 1988 Effects of radiotherapy on mandibular reconstruction plates *Am. J. Surg.* **156** 261–3

Cieslar J, Huang M T and Dobson G P 1998 Tissue spaces in rat heart, liver, and skeletal muscle *in vivo Am. J. Physiol.* **275** R1530–6

Dvorak H F, Nagy J A, Dvorak J T and Dvorak A M 1988 Identification and characterization of the blood vessels of solid tumors that are leaky to circulating macromolecules *Am. J. Pathol.* **133** 95–109

Herold D M, Das I J, Stobbe C C, Iyer R V and Chapman J D 2000 Gold microspheres: a selective technique for producing biologically effective dose enhancement *Int. J. Radiat. Biol.* **76** 1357–64

Hirsch L R, Stafford R J, Bankson J A, Sershen S R, Rivera B, Price R E, Hazle J D, Halas N J and West J L 2003 Nanoshell-mediated near-infrared thermal therapy of tumors under magnetic resonance guidance *Proc. Natl Acad. Sci.* **100** 13549–54

Matsudaira H, Ueno A M and Furuno I 1980 Iodine contrast medium sensitizes cultured mammalian cells to x-rays but not to γ rays *Radiat. Res.* **84** 144–8

Namito Y, Ban S and Hirayama H 1995 LSCAT: low-energy photon-scattering expansion for the EGS4 Code KEK Internal Document 95-10 (Tsukuba, Japan: KEK National Laboratory for High Energy Physics)

Nath R, Bongiorni P and Rockwell S 1990 Iododeoxyuridine radiosensitization by low- and high-energy photons for brachytherapy dose rates *Radiat. Res.* **124** 249–58

Nelson W R, Hirayama H and Rogers D W O 1985 The EGS4 Code System, SLAC 265

Norman A, Ingram M, Skillen R G, Freshwater D B, Iwamoto K S and Solberg T 1997 X-ray phototherapy for canine brain masses *Radiat. Oncol. Investig.* **5** 8–14

Pitsillides C M, Joe E K, Wei X, Anderson R R and Lin C P 2003 Selective cell targeting with light-absorbing microparticles and nanoparticles *Biophys. J.* **84** 4023–32

Regulla D F, Hieber L B and Seidenbusch M 1998 Physical and biological interface dose effects in tissue due to x-ray-induced release of secondary radiation from metallic gold surfaces *Radiat. Res.* **150** 92–100

Robar J L, Riccio S A and Martin M A 2002 Tumour dose enhancement using modified megavoltage photon beams and contrast media *Phys. Med. Biol.* **47** 2433–49

Rockwell S C, Kallman R F and Fajardo L F 1972 Characteristics of a serially transplanted mouse mammary tumor and its tissue-culture-adapted derivative *J. Natl Cancer Inst.* **49** 735–49

Rofstad E K and Brustad T 1985 Tumor growth delay following single dose irradiation of human melanoma xenographs: correlations with tumor growth parameters, vasculature structure, and cellular radiosensitivity *Br. J. Cancer* **51** 201–10

Rose J H, Norman A, Ingram M, Aoki C, Solberg T and Mesa A 1999 A first radiotherapy of human metastatic brain tumors delivered by a computerized tomography scanner (CTRx) *Int. J. Radiat. Oncol. Biol. Phys.* **45** 1127–32

Santos Mello R, Callisen H, Winter J, Kagan A R and Norman A 1983 Radiation dose enhancement in tumors with iodine *Med. Phys.* **10** 75–8

Spiers F W 1949 The influence of energy absorption and electron range on dosage in irradiated bone *Br. J. Radiol.* **22** 521–33